Journal of Nonlinear Optical Physics & Materials
Vol. 16, No. 3 (2007) 329–341

World Scientific
www.worldscientific.com

SYNTHESIS, CRYSTAL STRUCTURE, SPECTROSCOPIC STUDIES AND *AB-INITIO* CALCULATIONS ON THIRD-ORDER OPTICAL NONLINEARITY OF A FIVE-COORDINATE CHLOROIRON(III) COMPLEX

ASLI KARAKAS*

Department of Physics, Faculty of Arts and Sciences
Selçuk University, TR-42049 Campus, Konya, Turkey
karakasasli@yahoo.com

EMINE DONMEZ† and HULYA KARA‡

Department of Physics, Faculty of Arts and Sciences
Balikesir University, TR-10100 Campus, Balikesir, Turkey
†*donmezemine@hotmail.com*
‡*hkara@balikesir.edu.tr*

AYHAN ELMALI

Department of Engineering Physics, Faculty of Engineering
Ankara University, TR-06100 Tandoğan, Ankara, Turkey
Ayhan.Elmali@eng.ankara.edu.tr

Received 10 September 2007

A five-coordinate chloroiron(III) complex has been synthesized and characterized by X-ray diffraction analysis and UV-Vis spectroscopy. The maximum one-photon absorption (OPA) wavelengths recorded by both linear optical measurements and quantum mechanical computations using the configuration interaction (CI) method are estimated to be shorter than 400 nm in the UV region, showing good optical transparency to visible light. To investigate the microscopic third-order nonlinear optical (NLO) behavior of the title compound, we have computed both dispersion-free (static) and also frequency-dependent (dynamic) linear polarizabilities (α) and second hyperpolarizabilities (γ) at λ = 825–1125 nm and 1050–1600 nm wavelength areas using the time-dependent Hartree–Fock (TDHF) method. The *ab-initio* calculation results with non-zero values on (hyper)polarizabilities indicate that the synthesized molecule might possess microscopic third-order NLO phenomena.

Keywords: X-ray diffraction; UV-Vis; time-dependent Hartree–Fock; configuration interaction; third-order optical nonlinearity.

*Corresponding author. Permanent address: Department of Physics, Faculty of Arts and Sciences, Selçuk University, 42049 Campus, Konya, Turkey, E-mail address: karakasasli@yahoo.com (A. Karakas), Fax: +90 332 241 01 06.

1. Introduction

Although a great deal of work has been carried out on the investigation of the nonlinear optical (NLO) properties in organic molecules,[1] the optical nonlinearities of metal complexes have started to be actively studied more recently.[2,3] Metal-organic complexes have been extensively studied for the development of NLO materials owing to their rich electronic characters and structural variations.[4] The recent reports of structure-property relationships in metal-organic third-order NLO materials have clearly demonstrated that variations in both the metal and the ligands of these materials can have significant effects on their third-order NLO properties. Furthermore, with the proper combination of metal and ligands, metal-organic materials exhibit large second hyperpolarizabilities. An attractive feature of metal complexes as NLO materials is that molecular architectures can be easily modulated to optimize both the corresponding microscopic parameters as polarizability and hyperpolarizability, and the related macroscopic properties as susceptibility and thermal stability. Organic substituents and transition metal ions with unfilled *d*-shells influence the nonlinearity through the interaction between the electrons in the substituents and the electrons in the main organic system.[5] From the theoretical point of view, metal complexes have received less attention due to the difficulty in the calculation of hyperpolarizabilities in the presence of transition metal atoms. On the other hand, the use of semiempirical methods to calculate the NLO properties of metal complexes has been less reliable due to parametrization problems in the method of choice. Until now, however, the utilization of *ab-initio* methods to calculate the NLO characteristics of metal complexes has been exploited less, owing to the heavy computational cost in handling these systems.

Nonsubstituted or symmetrically substituted metal-organic complexes with centrosymmetric structures have basically been studied as third-order NLO materials.[6] Based on the structure and previous studies,[7] one could expect that the title iron(III) complex (Fig. 1) may show third-order NLO behavior. Theoretical calculations offer a quick and inexpensive way of predicting the NLO responses of the materials. In this paper, we have made an attempt to design a Schiff base metal complex and utilize *ab-initio* methods for investigating third-order NLO behavior. Therefore, we have characterized the newly synthesized title compound

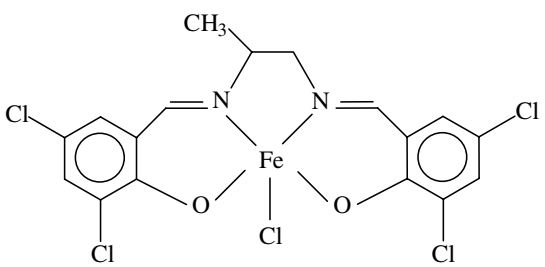

Fig. 1. The chemical structure of the title compound.

with spectroscopic (UV-Vis) and crystallographic (X-ray diffraction) techniques, and theoretically evaluated its third-order NLO response using the *ab-initio* time-dependent Hartree–Fock (TDHF) procedure on dispersion-free and frequency-dependent linear polarizabilities and second hyperpolarizabilities.

2. Experimental Section

2.1. *Reagent and techniques*

1,2-diamino propane, 3,5-dichlorosalicylaldehyde, $FeCl_3{\cdot}6H_2O$, methanol and ethanol were purchased from Aldrich Chemical Co.. Elemental (C, H, N) analyses were carried out by standard methods. UV-Vis spectra were measured using a Cary 1-E UV-Vis Spectrometer with 1.0 cm quartz cells.

2.2. *Preparation of the title complex*

1,2-diaminopropane (1 mmol) was slowly added to a solution of 3,5-dichlorosalicylaldehyde (2 mmol) in ethanol (100 ml) at 80°C. After stirring for 20 minutes, a yellow precipitate was collected by filtration. The compound was prepared by addition of 1 mmol of $FeCl_3.6H_2O$ in 40 mL of hot ethanol to 1 mmol of ligand in 100 mL of hot ethanol. The deep-green solution was filtered and taken to dryness. Crystals of the formulation were grown by slowly diffusing ether vapors into an acetonitrile solution. Several weeks of standing led to the growth of deep-green crystals of the title compound suitable for X-ray analysis. Found: C, 44.30%; H, 3.03%; N, 8.97%. $C_{40}H_{31}Cl_{10}Fe_1N_7O_4$; Calc. C, 44.32%; H, 2.88%; N, 9.04%.

2.3. *X-ray structure determination*

All geometric and intensity data were collected using three-circle CCD diffractometers equipped with graphite monochromated Mo K_α radiation ($\lambda = 0.71073$ Å) at −100°C. The intensity data were integrated using the SAINT[8] program. Absorption, Lorentz and polarization corrections were applied. The structures were solved by Direct Methods and refined using full-matrix least-squares against F^2 using SHELXTL.[9] All non-hydrogen atoms were assigned anisotropic displacement parameters and refined without positional constraints. Hydrogen atoms were included in idealized positions with isotropic displacement parameters constrained to 1.5 times the U_{equiv} of their attached carbon atoms for methyl hydrogens, and 1.2 times the U_{equiv} of their attached carbon atoms for all others. The 1,2-diaminopropane portion of the ligand showed positional disorder with two peaks, and the concerned carbon atom was refined as C(17a) and C(17b) with site occupancy factors of 0.70 and 0.30, respectively. Also, one of the acetonitrile molecules was disordered. The occupancies of the disordered positions were refined, keeping their sums as unity, the occupancies being fixed at 0.5. The higher R value (more than 0.1) might be due to the disorders of the acetonitrile molecule having a larger

thermal parameter for the nitrogen atom in the title compound. The crystallographic data, conditions used for the intensity data collection and some features of the structure refinement are listed in Table 1. Selected bond lengths and angles are summarized in Table 2. The chemical structure of the synthesized molecule is given in Fig. 1, and an ORTEP view of the molecular structure is shown in Fig. 2. Crystallographic data (excluding structure factors) for the structure reported in this paper have been deposited with the Cambridge Crystallographic Data Centre as supplementary publication no. CCDC 652094.[10]

Table 1. Crystallographic and refinement data for the title compound.

Formula	$C_{40}H_{31}Cl_{10}FeN_7O_4$
Formula weight	1139.92
Temperature	100(2) K
Wavelength	0.71073 Å
Crystal system	Monoclinic
Space group	$P2_1/c$
Unit cell dimensions	$a = 13.002(3)$ Å, $\alpha = 90°$ $b = 14.090(3)$ Å, $\beta = 102.04(3)°$ $c = 13.153(3)$ Å, $\gamma = 90°$
Volume	2356.5(2) Å^3
Z	2
Density (calculated)	1.606 mg·m^{-3}
Absorption coefficient	1.231 mm^{-1}
$F(000)$	1148
Theta range for data collection	2.14 to 27.49°
Index ranges	$-16 \leq h \leq 16$, $-18 \leq k \leq 18$, $-16 \leq l \leq 17$
Reflections collected	26016
Independent reflections	5392 [$R_{(\text{int})} = 0.1569$]
Refinement method	Full-matrix least-squares on F^2
Data/restraints/parameters	5392/0/311
Goodness-of-fit on F^2	0.945
Final R indices [$I \geq 2\sigma(I)$]	$R_1 = 0.0606$, $wR_2 = 0.1314$
R indices (all data)	$R_1 = 0.1324$, $wR_2 = 0.1575$
Largest diff. peak and hole [e. Å^{-3}]	0.827 and −0.829

Table 2. Some selected bond lengths [Å] and angles [°] for the title compound.

Fe(1)–O(1)	1.916(4)	Fe(1)–N(1)	2.097(4)
Fe(1)–O(2)	1.896(3)	Fe(1)–N(2)	2.100(4)
Fe(1)–Cl(1)	2.242(2)		
O(1)–Fe(1)–O(2)	96.99(1)	N(1)–Fe(1)–N(2)	77.37(2)
O(1)–Fe(1)–N(1)	85.98(2)	O(2)–Fe(1)–N(2)	86.87(2)
O(1)–Fe(1)–N(2)	152.29(2)	O(2)–Fe(1)–N(1)	149.34(2)
O(2)–Fe(1)–Cl(1)	107.71(1)	N(1)–Fe(1)–Cl(1)	101.59(1)
O(1)–Fe(1)–Cl(1)	100.93(1)	N(2)–Fe(1)–Cl(1)	103.98(1)

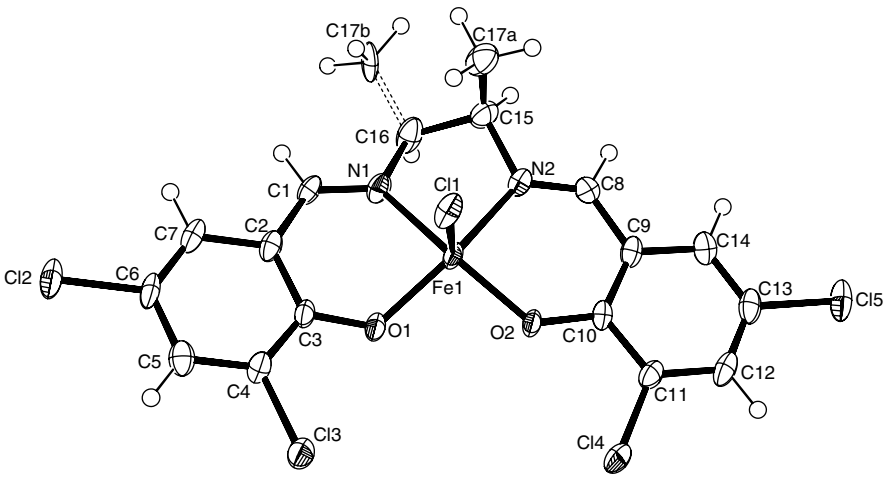

Fig. 2. The molecular structure of the components of the title compound. Displacement ellipsoids are plotted at the 50% probability level. Bonds to the disordered atoms C(17a) and C(17b) (see text) are shown. The solvent CH_3CN is omitted for clarity.

3. Theoretical Calculations

The theoretical computations involve the determination of dispersion-free and frequency-dependent linear polarizability and second hyperpolarizability tensor components of the title complex using the following methods:

As the first step of static and dynamic (hyper) polarizability calculations, the geometries taken from the starting structures in Table 2 have been optimized in the *ab-initio* restricted Hartree–Fock level. The optimized structures have been used to compute the linear polarizabilities and third-order hyperpolarizabilities at ω frequencies with a triple-zeta valence (code-named TZV) basis set, which is a kind of extended basis set.[11–13] The basis set effects are important for the calculation of NLO properties. Besides, while one computes the NLO properties for fairly large systems with transition metals, extended basis sets consisting of Gaussian-type functions are found to be especially important. Augmenting the basis set of elements with diffuse s, p and d functions in a proper way could provide the best compromise between speed and accuracy for the computation.[14] TZV basis set due to Dunning,[11] McLean *et al.*[12] and Wachters[13] has some contractions in the examined compound: [5s1p/3s1p] for H; [10s6p/5s3p] for C, N, O; [12s9p/6s5p] for Cl; [14s11p6d/10s8p3d] for Fe atoms. Contracted Gaussian basis sets of TZV quality are presented for Li to Kr, and then advantages and necessary modifications of them are discussed in the literature.[15] In general, TZV basis sets could be especially preferred when performing some quantum mechanical calculations of the compounds with transition metals using the *ab-initio* package GAMESS[16] at the Hartree–Fock level. Thus, it could be said that the TZV basis set is sufficient to compute the (hyper)polarizabilities of the title transition metal complex

with Fe center. $\alpha(0;0)$ and $\gamma(0;0,0,0)$ at $\omega = 0$; $\alpha(-\omega;\omega)$ and $\gamma(-3\omega;\omega,\omega,\omega)$ calculations at $\omega = 0.05512, 0.04050, 0.04336, 0.02848$ atomic units (a.u.) (i.e., at $\lambda = 825, 1125, 1050, 1600$ nm wavelengths), often used laser frequencies in third-harmonic generation (THG) measurements, have been carried out using the TDHF method implemented in the GAMESS[16] program. In these γ definitions mentioned above; the first describes the static third-order hyperpolarizabilities, the second represents the hyperpolarizability for frequency tripling, called the THG process. All (hyper)polarizability calculations have been performed on a PC with an Intel Pentium IV operator, 512 MB RAM memory and 1.7 GHz frequency using Linux PC GAMESS version running under Linux 7.3 environment.

In this study, the average linear polarizability $\langle\alpha\rangle$ and third-order hyperpolarizability $\langle\gamma\rangle$ values have been calculated using the following expressions, respectively[17]:

$$\langle\alpha\rangle = (\alpha_{xx} + \alpha_{yy} + \alpha_{zz})/3 \tag{1}$$

$$\langle\gamma\rangle = (1/5)[\gamma_{xxxx} + \gamma_{yyyy} + \gamma_{zzzz} + 2(\gamma_{xxyy} + \gamma_{xxzz} + \gamma_{yyzz})]. \tag{2}$$

Since the α and γ values of the GAMESS output are reported in a.u., the calculated α and γ values have been converted into the electrostatic units (esu) (1 a.u. $\alpha = 0.1482 \times 10^{-24}$ esu, 1 a.u. $\gamma = 5.0367 \times 10^{-40}$ esu). To calculate all the (hyper)polarizabilities, the origin of the cartesian coordinate system $(x, y, z) = (0, 0, 0)$ has been chosen at its own center of mass of the studied compound in Fig. 1.

Besides, the $\pi \rightarrow \pi^*$ transition wavelengths ($\lambda_{\max}$) of the lowest lying electronic transition and the oscillator strengths (f) of these transitions for the investigated molecule have been theoretically studied by electron excitation configuration interaction using the CIS/6-31G method in GAUSSIAN98W[18] on an Intel Pentium IV 1.7 GHz processor with 512 MB RAM and Microsoft Windows as the operating system.

4. Results and Discussion

4.1. *UV-Vis spectroscopy*

It can be very helpful in the investigation of NLO materials, making it possible to check, apart from NLO responses, also the spectroscopic absorbance in the appropriate wavelength. Therefore, the wavelengths obtained by UV-Vis spectral analysis can be helpful in planning the synthesis of only the promising NLO materials. Since it is necessary to know the transparency region, the electronic absorption spectral studies of compounds designed to possess NLO properties are important. Albert *et al.*[19] have reached the conclusion that with the correct substitution of the push-pull system in the porphyrin ring, characterized by strong intramolecular $\pi \rightarrow \pi^*$ charge transfer (CT) transitions found through UV-Vis spectral analysis, some specific electronic and structural properties of this system could produce

high NLO responses. Zhou *et al.*[20] have found that the λ_{max} results of novel paraphenylenealkyne macrocycles are not accelerated with the odd number of units, even with 10 units, the value of λ_{max} is 360 nm. Although the λ_{max} was estimated to be shorter than 400 nm in a large enough sample, a strong increase in the hyperpolarizability value is obtained with a sizeable increase. Di Bella *et al.*[21] have reported bis(salicyl-aldiminato) nickel(II) compound exhibiting interesting linear optical features which will be seen to be related to the NLO response. There is a broad band in the region between 300 and 360 nm involving mainly $\pi \rightarrow \pi^*$ transitions. Li and co-workers have found that the UV-Vis absorption spectrum of a manganese(II) coordination polymer displays two strong absorption peaks at 268 and 282 nm. The polymer exhibiting third-order optical nonlinearity has relatively low linear absorption in the UV and visible regions.[22] The UV-Vis spectra of the title complex have been recorded by the spectrometer in the range of 190–1100 nm. Figure 3 displays the linear absorption spectrum. The maximum absorption wavelengths λ_{exp} obtained from the UV-Vis spectral analysis in methanol solvent are listed in Table 3. The studied compound has three absorption bands in the near UV-Vis region below 400 nm, which is a dominant feature in the absorption spectrum. Near UV absorptions include quite intense $\pi \rightarrow \pi^*$ transitions. As seen in the spectra, there is no absorption above 400 nm, i.e., it remains transparent above 400 nm. The absence of the absorption above 400 nm in the visible regime might enable the achievement of microscopic NLO response with non-zero values.

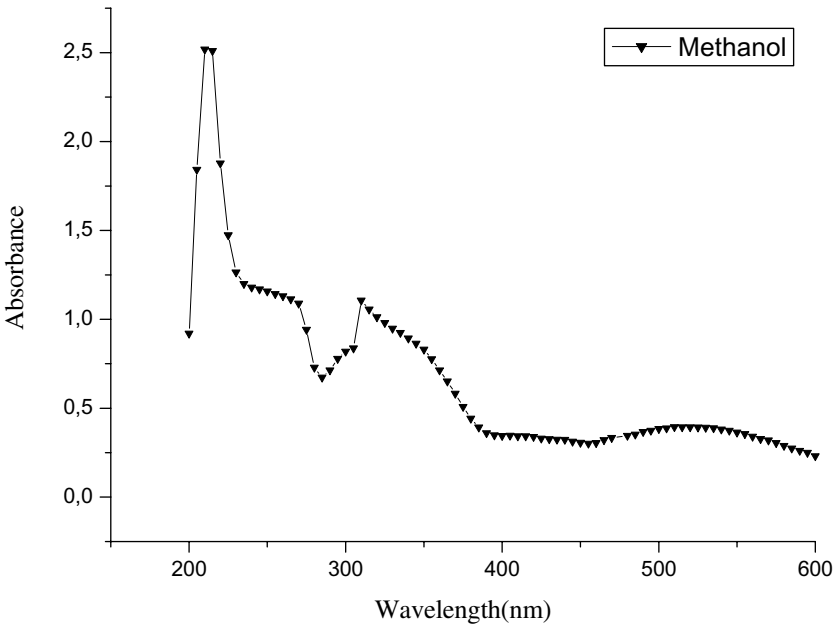

Fig. 3. UV-Vis absorption spectra of the title compound in methanol.

Table 3. Calculated and observed in methanol the maximum OPA wavelengths and oscillator strengths of the title compound.

λ_{max} (nm)	f	λ_{exp} (nm)
333.26	1.1766	310.1
291.02	1.4835	270.0
200.14	1.0008	210.0

4.2. *Description of the crystal structure*

The title compound contains one complex molecule and two isolated MeCN molecules. In the complex, the iron ion is in the +3 oxidation state and the coordination geometry around the metal centre is distorted square-pyramidal, which is common for five-coordinate salen-iron complexes.[23] The iron of the examined compound is coordinated two phenolate oxygens (O(1) and O(2)) and two imine nitrogens (N(1) and N(2)), as well as the chlorine atom (Cl(1)). Two terminal phenolic oxygens and imine nitrogens in *cis* positions are centered around iron(III). All the Cl(1)–Fe–N(l), Cl(1)–Fe–N(2), Cl(1)–Fe–O(l), and Cl(1)–Fe–O(2) angles are significantly larger than 90°, and the sum of the O(1)–Fe–N(1), N(l)–Fe–N(2), N(2)–Fe–O(2), and O(2)–Fe–O(1) angles are only 347.21°. The Fe(1)–Cl(1) bond is a little shorter than the corresponding distance of 2.306 (2) Å observed in another iron(III) complex.[24] The Fe–O bonds are longer than the corresponding distance of 1.890 (3) Å observed in Ref. 25. The iron(III)-imine nitrogen bond distances are characteristic in different structurally characterized Schiff base complexes, in the range of 2.00–2.10.[24] O(1)–Fe–N(2) and O(2)–Fe–N(1) *trans* angles lie in the value of 152.31° and 149.31°, respectively. The Fe(III) atom is situated 0.469 Å above the plane defined by the N_2O_2 ligand donor set whereas in Ref. 26, the iron atom is lying at 0.528 Å. The iron atoms are substantially protruded from the ligand plane, which represent the typical five-coordinate square-pyramidal arrangement.[27] The dihedral angle between the planes defined by O(1)–Fe–N(1) and N(2)–Fe–O(2) is 37.70°. Atoms C(15) and C(16) deviate from the Fe(1)–N(1)–N(2) plane by 0.448 and 0.126 Å, respectively.

4.3. *Computational results and discussion*

The incorporation of a heavy atom introduces more sublevels into the energy hierarchy as compared to organic molecules with the same number of skeletal atoms, and this permits a greater number of allowed electronic transitions and hence enhances the NLO effects. The central metal atom of a metal complex can readily coordinate to conjugated ligands and undergo π-orbital overlap facilitating effective electronic communication. Moreover, metals can have a large diversity of coordination mode with various organic ligands, and changing a ligand in the coordination sphere can affect the function of the metal fragment, and thus nonlinear activity. Since the potential of organic materials and metal complexes for NLO devices have been

proven, the NLO properties of many of these compounds have been investigated by both experimental and theoretical methods.[28] In the past five years, the efforts on NLO have been devoted to preparing third-order NLO materials using theoretical methods and exploring the structure-property relationships. Quantum chemical calculations have been shown to be useful in the description of the relationship between the electronic structure of the systems and its NLO response.[29] The computational approach allows the determination of molecular NLO properties as an inexpensive way to design molecules by analyzing their potential before synthesis and to determine high-order hyperpolarizability tensors of molecules.

In this paper, the vertical transition energies and oscillator strengths from the ground state to each excited state have been computed, giving OPA, i.e., the UV-Vis spectrum. The calculated wavelengths ($\lambda_{\max}$) and oscillator strengths (f) for the maximum OPA of the investigated molecule are shown in Table 3. The molecule in Fig. 1 has three OPA peaks in its spectrum. As can be seen from Table 3, the optical spectra exhibit three relatively intense bands involving $\pi \rightarrow \pi^*$ transitions centered between 200 and 333 nm. The values of all absorption maxima are located in the UV region estimated to be shorter than 400 nm, being transparent in the visible region.

In spite of the rapid development of highly advanced experimental techniques on NLO, the theoretical understanding of the NLO properties show that the responses of the molecule to the external application of an electric field are also of much importance. One could determine the hyperpolarizability tensors of molecules using a suitable computational approach. These tensors describe the response of molecules to an external electric field. It is known that there are several well-established computational procedures that include correlation at various levels of rigor, and are used for the computation of NLO properties. At the molecular level, the NLO properties are determined by their dynamic hyperpolarizabilities. TDHF is a procedure generally used to find out approximate values, and can be a means of understanding both the static and dynamic hyperpolarizabilities of organic molecules. We present here a comprehensive *ab-initio* study on the NLO properties of the title molecule using the TDHF method. In this study, in addition to the static linear polarizabilities $\alpha(0;0)$ and second hyperpolarizabilities $\gamma(0;0,0,0)$, the following processes for dynamic (hyper)polarizabilities have been considered: frequency-dependent linear polarizabilities $\alpha(-\omega;\omega)$, THG $\gamma(-3\omega;\omega,\omega,\omega)$. Some significant calculated magnitudes of the static and frequency-dependent linear polarizabilities and second hyperpolarizabilities are shown in Tables 4–7, respectively.

Table 4. Some selected components of the static $\alpha(0;0)$ and $\langle\alpha\rangle$ $(0;0)$ [$\times 10^{-24}$ esu] value of the title compound.

α_{xx}	α_{yy}	α_{zz}	$\langle\alpha\rangle$
41.737	14.402	5.445	20.528

Table 5. Some selected components of the frequency-dependent $\alpha(-\omega;\omega)$ and $\langle\alpha\rangle$ $(-\omega;\omega)$ [$\times 10^{-24}$ esu] values at ω [in a.u.] laser frequencies for the title compound.

	$\omega = 0.05512$	$\omega = 0.04050$	$\omega = 0.04336$	$\omega = 0.02848$
α_{xx}	37.416	27.526	33.508	51.807
α_{yy}	8.549	14.318	15.195	15.618
α_{zz}	4.485	3.386	3.928	6.078
$\langle\alpha\rangle$	16.817	15.077	17.544	24.501

Table 6. All static $\gamma(0;0,0,0)$ components and $\langle\gamma\rangle$ $(0;0,0,0)$ [$\times 10^{-37}$ esu] value for the title compound.

γ_{xxxx}	γ_{yyyy}	γ_{zzzz}	γ_{xxyy}	γ_{xxzz}	γ_{yyzz}	$\langle\gamma\rangle$
15854.500	541.571	7.738	477.480	181.920	174.989	3614.518

Table 7. Some selected components of the frequency-dependent $\gamma(-3\omega;\omega,\omega,\omega)$ and $\langle\gamma\rangle$ $(-3\omega;\omega,\omega,\omega)$ [$\times 10^{-37}$ esu] values at ω [in a.u.] laser frequencies calculated with THG process for the title compound.

	$\omega = 0.05512$	$\omega = 0.04050$	$\omega = 0.04336$	$\omega = 0.02848$
γ_{xxxx}	19371.003	53879.734	6725.570	−55537.395
γ_{yyyy}	2989.746	184.618	−89.573	−473.096
γ_{zzzz}	420.379	49.542	316.434	572.296
γ_{xxyy}	23208.120	3044.665	1.847	−3579.965
γ_{xxzz}	881.605	4453.485	526.909	320.956
γ_{yyzz}	−24.416	373.005	55.579	108.446
$\langle\gamma\rangle$	8646.025	12594.586	1550.075	−14399.392

π-conjugated molecules with a donor and an acceptor will not display second-order NLO activity if they possess a center of symmetry. Unfortunately, the title compound has crystallized out in the monoclinic $P2_1/c$ space group, which is a centrosymmetric space group so that it does not exhibit second-order NLO properties. However, such centrosymmetric molecules might have third-order optical nonlinearity like the compound studied here. γ values depend on a number of factors, which include the extent of π electron conjugation, the dimensionality of the molecules and the nature of substituents. The introduction of transition metals with partially filled *d*-shells is known to affect a number of CT mechanisms such as metal-ligand charge transfer (MLCT), ligand-metal charge transfer (LMCT) and *d*-*d* charge transfer.[30] Besides, iron is a transition metal ion with a partially filled *d*-shell, which is also in favor of higher values of γ. The role of the metal center in determining the NLO response in π-conjugate metal complexes might be two-fold, since it can act either as the donor or the bridging moiety of the donor-(π-conjugate- bridge)-acceptor system. However, in the presence of strong donor-acceptor substituents, the metal mostly acts as a bridge. In particular, the low energy CT feature may be characterized as principally $\pi \rightarrow \pi^*$ in character, essentially involving the metal d_{xy}+O_{2py} and the C=N orbitals, and is mainly responsible

for the dispersion-free and frequency-dependent second hyperpolarizabilities with non-zero values (see Tables 6–7) as microscopic NLO response of the investigated molecule. In addition, the involvements of iron(III) ion with d^5 electron structure and electron rich acceptor −Cl atoms in the complex result in obvious enhancement of all the second molecular hyperpolarizabilities. The values of γ depend on the halogen substitution in the molecular structure. Further, the donor capacities of −Cl atoms are ordered in terms of their σ donation ability. Hence, one would expect the chloro compounds to exhibit larger second hyperpolarizabilities. The fact is that we observe that σ donation may not be the only role on γ values for halogens. An alternative model to explain this trend is based on the π donation ability of the halogen atom in the presence of π accepting ligands. This changes γ in these complexes. The better π donor capability of the investigated complex is based on the better π overlap of the $3d$ transition metal with the $3p$ orbitals of Cl(1) (Fig. 2). It is also important to stress that, in these α and γ investigations, we do not take into account the effect of the field on the nuclear positions, i.e., we evaluate only the electronic components of $\langle\alpha\rangle$ and $\langle\gamma\rangle$.

5. Conclusions

The title iron(III) transition metal complex has been synthesized, and its structural characterization has been investigated by X-ray diffraction measurements. The OPA characterization has been obtained both theoretically (CI method) and experimentally (UV-Vis spectroscopy). According to the calculation and measurement results on the linear optical behavior, the values of electronic transition wavelengths are estimated to be shorter than 400 nm, implying good optical transparency in the visible and near-IR region (400–900 nm). It is especially essential to know theoretically the frequency-dependence of second hyperpolarizabilities at the laser frequencies often employed in the THG measurements. We have presented the computational studies showing how the examined molecule can possess the third-order optical nonlinearity. The *ab-initio* calculated non-zero (hyper)polarizabilities suggest that the synthesized complex might have microscopic third-order NLO behavior.

Acknowledgments

This work was supported by the Turkish State of Planning Organization (DPT), TUBITAK and Selçuk University under grant numbers 2003-K-12019010-7, 105T132, 2003/030, respectively. Hulya Kara also thanks TUBITAK TBAG-2307 (103T041) for financial support, the NATO-B1-TUBITAK for funding and Prof. Guy Orpen (School of Chemistry, University of Bristol, UK) for his hospitality.

References

1. A. Karakas, H. Unver and A. Elmali, *Journal of Nonlinear Optical Physics & Materials (JNOPM)* **16**(1) (2007) 91.

2. A. Elmali, A. Karakas and H. Unver, *Chem. Phys.* **309** (2005) 251.
3. A. Karakas, H. Unver and A. Elmali, *J. Mol. Struct. (Theochem)* **774** (2006) 67.
4. D. M. Roundhill and J. P. Fackler Jr., *Optoelectronic Properties of Inorganic Compounds* (Plenum Press, New York, 1999).
5. P. Romaniello and F. Lelj, *J. Fluorine Chem.* **125** (2004) 145.
6. J. S. Shirk, J. R. Lindle, F. J. Bartoli, C. A. Hoffman, Z. H. Kafafi and A. W. Snow, *Appl. Phys. Lett.* **55** (1989) 1287.
7. A. Karakas, H. Unver, A. Elmali and I. Svoboda, *Z. Naturforsch.* **60a** (2005) 376.
8. *SMART, SAINT and SHELXTL* (Bruker AXS Inc., Madison, Wisconsin, USA, 2002).
9. G. M. Sheldrick, *SADABS* (University of Göttingen, Göttingen, Germany, 2003).
10. CCDC 652094 contains the supplementary crystallographic data for this paper. These data can be obtained free of charge via www.ccdc.cam.ac.uk/data_request/cif, or by emailing data_request@ccdc.cam.ac.uk, or by contacting The Cambridge Crystallographic Data Centre, 12, Union Road, Cambridge CB2 1EZ, UK; fax: +44 1223 336033.
11. T. H. Dunning, *J. Chem. Phys.* **55** (1971) 716.
12. A. D. McLean and G. S. Chandler, *J. Chem. Phys.* **72** (1980) 5639.
13. A. J. H. Wachters, *J. Chem. Phys.* **52** (1970) 1033.
14. G. Maroulis, D. Xenides, U. Hohm and A. Loose, *J. Chem. Phys.* **115** (2001) 7957.
15. A. Schäfer, C. Huber and R. Ahlrichs, *J. Chem. Phys.* **100** (1994) 5829.
16. Intel×86 (win32, Linux, OS/2, DOS) version. PC *GAMESS* version 6.2, build number 2068. This version of *GAMESS* is described in: M. W. Schmidt, K. K. Baldridge, J. A. Boatz, S. T. Elbert, M. S. Gordon, J. H. Jensen, S. Koseki, N. Matsunaga, K. A. Nguyen, S. J. Su, T. L. Windus, M. Dupuis and J. A. Montgomery, *J. Comput. Chem.* **14** (1993) 1347.
17. M. P. Bogaard and B. Orr, Physical Chemistry, Molecular Structure and Properties, in *MTP International Review of Science*, ed. A. D. Buckingham, Vol. 2 (Butterworths, London, 1975), p. 149.
18. M. J. Frisch, G. W. Trucks, H. B. Schlegel, G. E. Scuseria, M. A. Robb, J. R. Cheeseman, V. G. Zakrzewski, J. A. Montgomery, Jr., R. E. Stratmann, J. C. Burant, S. Dapprich, J. M. Millam, A. D. Daniels, K. N. Kudin, M. C. Strain, O. Farkas, J. Tomasi, V. Barone, M. Cossi, R. Cammi, B. Mennucci, C. Pomelli, C. Adamo, S. Clifford, J. Ochterski, G. A. Petersson, P. Y. Ayala, Q. Cui, K. Morokuma, D. K. Malick, A. D. Rabuck, K. Raghavachari, J. B. Foresman, J. Cioslowski, J. V. Ortiz, A. G. Baboul, B. B. Stefanov, G. Liu, A. Liashenko, P. Piskorz, I. Komaromi, R. Gomperts, R. L. Martin, D. J. Fox, T. Keith, M. A. Al-Laham, C. Y. Peng, A. Nanayakkara, C. Gonzalez, M. Challacombe, P. M. W. Gill, B. Johnson, W. Chen, M. W. Wong, J. L. Andres, C. Gonzalez, M. Head-Gordon, E. S. Replogle and J. A. Pople, *GAUSSIAN98*, Revision A.7 (Gaussian Inc., Pittsburgh, PA, 1998).
19. I. D. L. Albert, T. J. Marks and M. A. Ratner, *Chem. Mater.* **10** (1998) 753.
20. Y. Zhou, S. Feng and Z. Xie, *Opt. Mater.* **24** (2003) 667.
21. S. Di Bella, I. Fragalà, I. Ledoux, M. A. Diaz-Garcia, P. G. Lacroix and T. J. Marks, *Chem. Mater.* **6** (1994) 881.
22. Y. Li, Z.-X. Zhang, F.-Y. Fang, W.-D. Song, K.-C. Li, Y.-L. Miao, C.-S. Gu and L.-Y. Pan, *J. Mol. Struct.* **837** (2007) 269.
23. H. Fujii and Y. Funahashi, *Angew. Chem. Int. Ed.* **41** (2002) 19.
24. Z. L. You and H. L. Zhu, *Acta Cryst.* **E60** (2004) 1046.
25. M. Lubben, A. Meetsma, F. Bolhuis and B. L. Feringa, *Inorg. Chim. Acta* **215** (1994) 123.
26. K. Oyaizu and E. Tsuchida, *Inorg. Chim. Acta* **355** (2003) 414.

27. M. Gerloch and F. E. Mabbs, *J. Chem. Soc. A* (1967) 1598.
28. H. S. Nalwa, M. Hanack, G. Pawlowski and M. K. Engel, *Chem. Phys.* **245** (1999) 17.
29. D. M. Burland, R. D. Miller and C. A. Walsh, *Chem. Rev.* **94** (1994) 31.
30. K. P. Unnikrishnan, J. Thomas, V. P. N. Nampoori and C. P. G. Vallabhan, *Synthetic Met.* **139** (2003) 371.